The dynamics of vortex structures and states of current in plasma-like fluids and the electrical explosion of conductors: III. Comparison with experiment

1993 J. Phys. A: Math. Gen. 26 6667

(http://iopscience.iop.org/0305-4470/26/23/016)

J. Phys. A: Math. Gen. 26 (1993) 6667–6677. Printed in the UK

The dynamics of vortex structures and states of current in plasma-like fluids and the electrical explosion of conductors: III. Comparison with experiment

N B Volkov and A M Iskoldsky
Russian Academy of Science, Ural Division, Institute of Electrophysics,
34 Komsomolskaya St., Yekaterinburg 620219, Russia

Received 4 September 1992, in final form 20 September 1993

Abstract. This paper is the concluding paper in a series of three. On the basis of the results of the first two, the experiments on the electric explosion in conductors are discussed and the mechanism of 'hot' plasma spot formation, which was observed repeatedly in the experiments on plasma focus, z-pinches, vacuum sparks and electric explosion of microwires, has been proposed. To realize this mechanism, the formation of sausage-type instabilities is not necessary. Moreover, the possibility of the formation of hot spots in a liquid metal (in the model under discussion, the plasma-like medium is assumed to be incompressible with constant local kinetic transport coefficients) has been shown. The latter is of great interest for understanding the mechanism of initiation and operation of vacuum arc cathode spots and also for the explanation of the phenomenon of explosive electron emission, which is widely employed in applied physics.

1. Introduction

In the present paper, which is the third part of a series [1, 2], we confine ourselves to a comparison with old experiments on the electric explosion of conductors (EEC), which represent a large volume of experimental data [3–5]. They contain a considerable number of facts, known as anomalies of electric explosion, which have not yet found a satisfactory interpretation. Closely related to this problem are papers on liquid-metal current interrupters, z-pinches [6], plasma focus experiments [7] and plasma-erosion current breakers [8].

2. Experimental techniques

For a more objective discussion of the experimental data on EEC, let us review experimental techniques (this problem has a more detailed consideration in [3–5]). The major experiments discussed below were carried out with the RLC circuit corresponding to the circuit S3 in [2] without the load resistor R (reference [2] figure 1(c)), on the basis of high-voltage (U_C = 50 kV), low-inductive capacitors with total capacitance (2.5–8) μF. The initial charge voltage ranged from 10 to 50 kV and the period of oscillations was between 5 and 40 μs. The maximum current amplitude was limited to 100 kA. The accuracy of the initial charge voltage was about 10^{-3}. In most experiments the initial parameters were adjusted so that the stage of conductor melting began within the maximum of the first half-cycle of a current wave in the RLC circuit. A typical value of the current density (j) for this type of source is about 2×10^7 A cm^{-2}.

0305-4470/93/236667+11$07.50

A three-channel square-wave generator made of 50 Ω, RF cables [9] was used to obtain maximal current densities of $(1–5)\times10^8$ A cm^{-2}. The pulse rise time was 1 ns. One of the generator channels was connected to the load and the other two served to control the electron–optical image converter. In the load capacitor the authors [4, 9] used a microwire of 10 μm in diameter and several mm in length.

The experiments dealt mostly with two observables: the total current, measured with the help of a special shunt, and the voltage, measured by a compensated Ohmic divider installed parallel to the conductor. The signals were recorded using fast oscilloscopes with a bandwidth of 3 GHz or a rapid double-channel digitizer with a sampling time of 7 ns and an amplitude resolution of 1%.

Furthermore, images of the exploding conductor were taken by electron–optical and by pulse shadow x-ray photography. The picture quality in x-ray photographs obtained in [4] is characterized by the following figures: the lack of sharpness of the image edge is of the order of 20 μm, the number of allowed shadings is more than 10, the minimum allowed thickness is of the order of 50 μm of Al and the maximum is of the order of 1 mm of Cu, the accuracy of timing photographs to voltage waveforms is within 2×10^{-8} s^{-1}.

Effective methods of obtaining and processing the experimental data allowed us to find insignificant (of the order of a few percent) changes in the data caused by physical fluctuation processes. For instance, registered with a high level of significance was a change within 10% of the slope of resistivity against absorbed energy (in the stage preceding melting) and also, under similar conditions, a shift of coordinates of the initial melting point by about 10% [4].

3. Discussion

In most experiments (see [3, 5]) only two signals are usually measured: the total current and voltage drop across the conductor. Therefore, below, we discuss basically the experiments of [4], where, in addition to the measurements mentioned above, shadow x-ray photography and photography by an electron–optical image converter were used.

Figure 1 shows typical waveforms of the current (figure 1(a)) and the voltage drop (figure 1(b)) without an inductive component. Shown in figure 1(c) is the time variation of the relative conductor radius taken by shadow x-ray photography. The initial point of an electric explosion on the current curve is practically indistinguishable, though on the voltage curve it is marked by an increase in the voltage growth rate. However, the transition region is sufficiently wide. Therefore it is not simple to determine the initial explosion point by the current and voltage waveforms. Independent measurements of the conductor radius during the explosion enables removal of the ambiguity (the change in the mechanism of conductor expansion takes place at the initial explosion point (figure 1(c))).

The ratio of a voltage signal to the current is interpreted as the conductor resistance, their product as the absorbed power, and the integral of this product over time as the absorbed energy. This interpretation is based on *a priori* assessments of a characteristic time of the magnetic field diffusion. This time is shorter than the characteristic time of the change in current and for these reasons the current density as well as other parameters are assumed to be evenly distributed over the conductor volume. By using the dependence on time and absorbed energy found in this way, one can determine parameters corresponding to the initial explosion point: the time (t_c) and the absorbed energy $Q(t_c)$.

The latter quantities have been widely discussed in the literature [3]. The authors of [3, 10] state that $Q(t_c)$ is independent of the current density, i.e. of the conductor heating

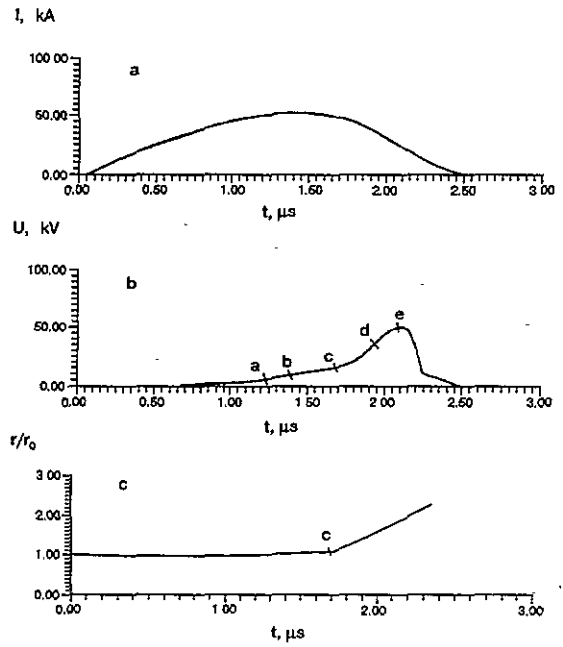

Figure 1. (*a*) Current, (*b*) voltage waveforms and (*c*) the radius as a function of time, obtained during the electric explosion of a copper wire 0.4 mm in diameter and 10 cm long. Circuit parameters: $C = 4.2$ μF, $L = 16$ nH, $U = 30$ kV [4]. The curve $u(t)$ (*b*) features the following typical points: 'a' the start of melting (t_a); 'b' the end of melting (t_b); 'c' the onset of the explosion (t_c); 'd' the maximal rate of the voltage growth (t_d); 'e' the maximal voltage (t_e).

rate, if the conductor is homogeneous over the radius ($t_c \gg r_0 c_s^{-1}$, where r_0 and c_s are the conductor radius and the sound velocity, respectively). Moreover, they suggest defining the initial explosion point as a point corresponding to the same resistance of a conductor made of the same material (e.g. for W the resistance (R_{eff}) with $t = t_c$ equal to the resistance at the end of melting is chosen in [10]), or as a point corresponding to the time when the condition $v(t)v_0^{-1} = 1.35$–1.45 (v and v_0 are the instantaneous and initial volumes of the conductor, respectively) is satisfied [3]. This estimate calculated for the radius has the form $r_c = r(t_c) = (1.162$–$1.204)r_0$. The lower estimate is in good agreement with the experimental results of [4] (figure 1(*c*)).

In order to check the hypothesis of $Q(t_c)$ dependence on the current density and the linear dependence of $R_{eff}(Q)$ in section b–c in figure 1, we simulated this situation in circuit S2 of our paper [2] where we calculated the process with two values of the dimensionless load impedance (Π_3): $\Pi_3 = 1$ and $\Pi_3 = 4$ (figure 2(*a*)–(*c*)). It can be seen that $R_{eff}(Q)$ in this section may be approximated by a linear dependence, the resistance corresponding to a higher energy input rate into the conductor being in the region of a high absorbed energy. From the results of our calculations, we can suggest the following about the parameters of the initial explosion point. If, similar to [3, 10], we assume $Q(t_c)$ is independent of the energy input rate, then for the above value we should take a point with $Q = 1.71 \times 10^{-1}$ and $t \cong 10.1$ in figure 2(*a*) (the units of measurement are relative), which is located far from the region of a sharp increase in R_{eff}. According to figure 1(*c*), however, the initial explosion point localizes at the beginning of the region of a fast R_{eff} increase. In analysing figure 2 one should bear in mind that in our model the fluid is considered to be incompressible and kinetic coefficients to be constant. In addition, the growth of R_{eff} is determined not by the dependence of electric conductivity on temperature but by the dynamics of vortex states, which result in the fact that an unperturbed state with an evenly distributed current density over the conductor radius is essentially disturbed. As a result, it is not only the current density that is unevenly distributed over the conductor but the temperature as well. Due to

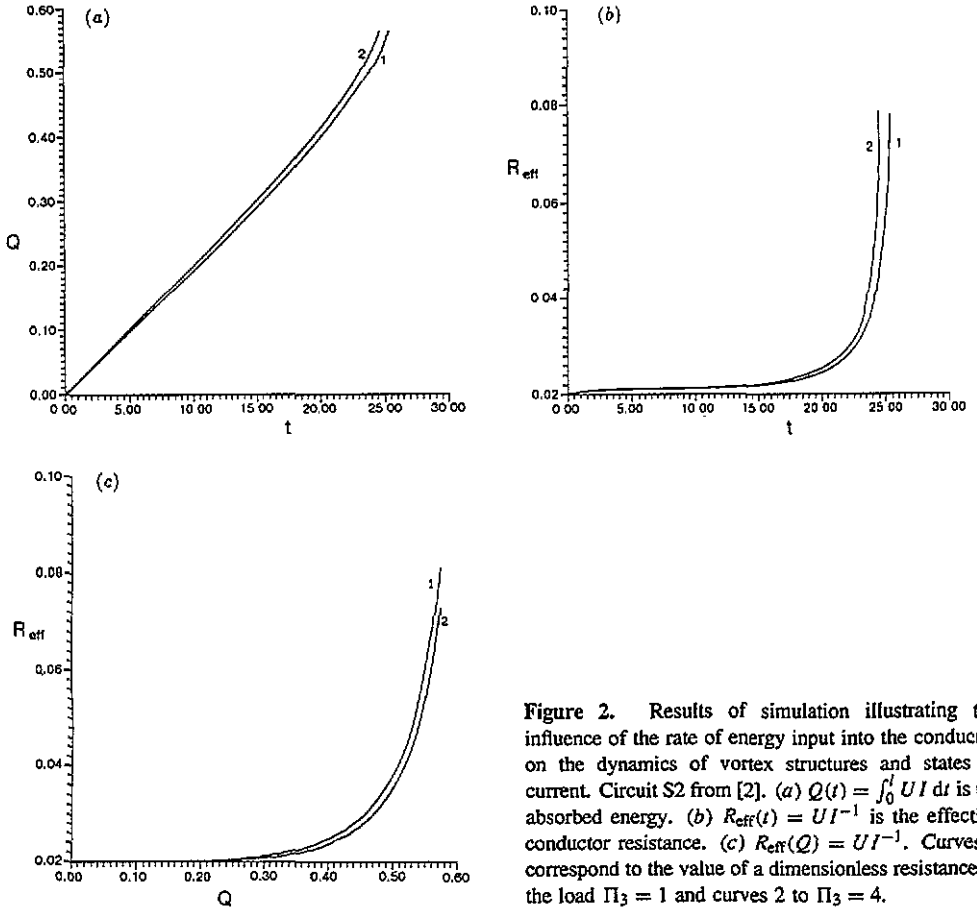

Figure 2. Results of simulation illustrating the influence of the rate of energy input into the conductor on the dynamics of vortex structures and states of current. Circuit S2 from [2]. (*a*) $Q(t) = \int_0^t UI\,dt$ is the absorbed energy. (*b*) $R_{\text{eff}}(t) = UI^{-1}$ is the effective conductor resistance. (*c*) $R_{\text{eff}}(Q) = UI^{-1}$. Curves 1 correspond to the value of a dimensionless resistance of the load $\Pi_3 = 1$ and curves 2 to $\Pi_3 = 4$.

this fact, one of the anomalies of the electric explosion is removed, namely the problem of the conductor overheating (see below). Moreover, the interpretation of experiments based on *a priori* assessments of a short diffusion time can be assumed to be misleading.

An essential feature of the electric explosion in conductors is their critical (threshold) character. The model discussed has a natural criterion (the magnetic Rayleigh number) and the question of whether the explosion transition has to occur is solved positively, at least for the source of an infinite power, if this parameter surpasses a critical value defined by the geometry and the conductor properties. For the source with a finite energy content, as pointed out in [2], the situation is more complex. In this case, the question of whether the explosion has to occur is determined not only by the control parameter r_1, which equals the ratio of the magnetic Rayleigh number to the critical one, but also by the initial level of fluctuations in the system given by the amplitudes $X(t)$, $Y(t)$ and $Z(t)$ (X belongs to mechanical degrees of freedom and Y and Z to electromagnetic ones). Our model is applicable from time t_0, which corresponds to the end of the conductor melting. The experiment in [4] shows that the initial and final melting points shift towards the region of a high absorbed energy where the values of R_{eff} and the slope angle $R_{\text{eff}}(Q)$ are smaller than the table values. Moreover, the same experiment shows that the resistance of a wire made of such materials as steel, tungsten and molybdenum decreases with increasing Q. Therefore when comparing our model with experiment, there arises the problem of not only

finding a critical value of the control parameter r_1 but also defining the initial data. It can easily be shown that by choosing the value of Z_0, one can obtain a decrease in R_{eff} and by choosing X_0 a shift towards the region of a high absorbed energy can be obtained.

Experiments in [11] have shown that if the current is rapidly interrupted before the conductor is brought up to its melting point, then the conductor is destroyed after about 200 μs. In a similar way, when the current is interrupted before the conductor reaches its melting point, the conductor starts bending after some delay time. In [12], for a Cu conductor 1 mm in diameter, the delay time was about 100 μs. In [4], bending in the central section of the conductor forms when the absorbed energy corresponds to that for liquifaction of the metal. This indicates that, on the one hand, the wavelength of the instability due to bending is apparently fixed when the conductor material is elastic and, on the other hand, that the melt can resist shearing stress at least during a few microseconds after it has been produced. In terms of our model (see [1]), the formation of vortex hydrodynamical structures introduces elements of a solid into the fluid: the effective voltage tensor is non-diagonal and the fluid gains in its ability to resist deformation. It should be noted that vortex excitations are similar to disclinations in liquid and solid crystals. Therefore the development of calibration continuous models of defects (dislocations and disclinations), which interact with the electromagnetic field of the model type proposed in [13], represents an up-to-date problem in the study of pulse heating and melting of conductors exposed to heating by current. These models will enable not only the explanation of destruction after the interruption of current but also the solution of the problem of the starting level of disbalance for the liquid-metal stage.

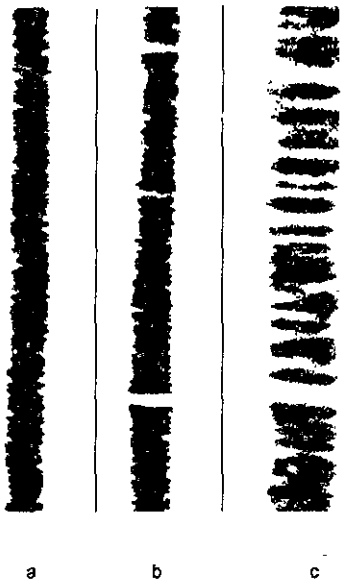

Figure 3. X-ray photograph of the conductor cross section at various times: 'a' corresponds to the time t_c, 'b' to t_d and 'c' to t_e, obtained during the explosion of a copper wire 0.58 mm in diameter. Circuit parameters: period 40 μs, capacitance $C = 4.2$ μF and initial voltage $U = 30$ kV [4].

One of the most indicative features of the electric explosion is the emergence of a characteristic large-scale band-like structure or strata dividing the conductor into lengths of a typical size close to the initial radius of the conductor (figure 3; see also figure 2 in [1]). Shown in figure 3 are the data of explosion for a Cu conductor 0.58 mm in diameter in an electric circuit with period 40 μs, storage capacitance 4.2 μF and initial voltage 30 kV. The

voltage rise time from the starting point of the explosion to the maximum value (points 'c' and 'e', figure 1(*a*)) was 1.2 μs. The fast current interruption phase lasted 1 ms and the time of the second phase (from the inflection point on the leading edge (figure 1(*a*), point 'd') to the point 'e') was about 200 ns. The first picture of figure 3 shows the beginning of the first phase, the second picture was taken at its end and the third one near the maximum of the voltage pulse. In the first picture one can see an axially asymmetric, small-scale structure with a typical size of about 0.3 mm. In the second picture, in at least three locations, plasma strata have already been formed. The third picture is a typical pattern of a fully stratified conductor. The mean distance between the strata is 0.78 mm, and it is twice as large as the small-scale structure at the beginning of the first phase. In addition, it appears that the typical size in the first approximation is independent of the experimental conditions, and the time to form this structure may be shorter than the typical sound time (it follows from the comparison of the last two pictures in figure 3, that the stratification process of the experiment discussed lasted 200 ns).

In the framework of our model the structure size is set by the wavenumber of the most rapidly increasing harmonic, and in accordance with the analysis in [1] for a Cu conductor 0.58 mm in diameter, it has to be $l = 2\lambda = 0.672$ mm. In the experiment from [4] discussed above, we have a value very close to $l = 0.78$ mm. If we employ the radius value corresponding to the initial explosion point from [3] $r(t_c) \cong 1.162r_0$, close to the experimental data from [4], we find a better agreement with experiment: $l = 0.781$ mm. Moreover, in later phases of the instability development one can observe the coalescence of adjoining strata into pairs (see figure 2 in [1]).

Such fine effects are predicted by the model: the harmonic with wavenumber $0.5k$, according to figure 1 from [1], has to be excited by the following one. To help understand the pairing effect discussed, consider the well known result of vortex system dynamics:

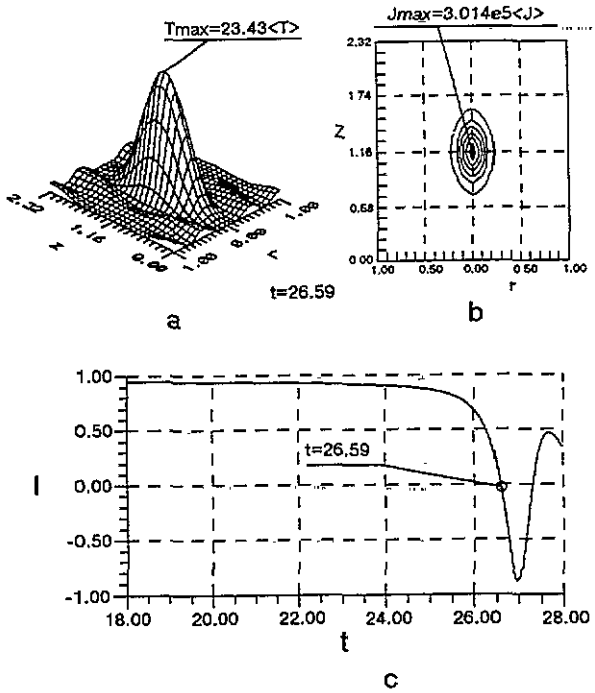

Figure 4. (*a*) Spatial distribution of the temperature, (*b*) the radiation and (*c*) the current curve, obtained by simulation of the circuit S2 in [2]. The time for the plots in (*a*) and (*b*) is marked on the current curve.

two vortex rings are either attracted or repelled (depending on the relative orientation of the particle rotation near the axis of vortex rings) [14]. The contact point between two repelling vortices can move from the external surface deep into the interior at a speed well above that of sound, because the movement is of a phase nature (in [15] we developed a three-mode model of this stage of the process, which is similar to the model discussed here and where the X, Y and Z amplitudes have the asymptote $X \sim Y \sim Z \sim (t_* - t)^{-1/2}$).

At the beginning of the conductor destruction, the energy deposited in it is sufficient to heat the conductor up to a temperature well above (by 2–3 times) the boiling point on the assumption that the temperature distribution is practically uniform over the volume. The experimental lifetime of this state is several orders of magnitude higher than the most radical estimations derived from the usual theory (e.g. by Frenkel–Zeldovitch–Folmer [16]). The difficulty mentioned is absent from the model under discussion: in our case, because the temperature distribution over the conductor volume is essentially non-uniform. The maximum temperature can be well above the mean value and the surface temperature can be well below the mean value over the volume (see figure 4(a)). In our case, $T_{\max} = 23.43\langle T \rangle$ ($\langle \cdot \rangle$ denotes volume average).

The maximum x-ray intensity corresponds to the local temperature maximum (figure 4(b); the time used for the plots in figure 4(a), (b) is marked in the current curve (c)). These regions of high temperature are detected by a pinhole chamber and interpreted as the so-called hot plasma spots (see [17] and also [18–20]). The generally accepted theory assumes that hot spots form as a result of sausage-type instabilities (micro-pinches) caused by radiation cooling and the escape of particles of matter from the region of the sausage-type instability [21]. In our case, the self-focusing of current occurs not due to 'raking up' of matter but to the decrease in the cross section of the channel, along which a laminar component of current flows (see figure 9 in [2], which shows cross sections of separatrix surfaces in the field of current velocities of conduction electrons).

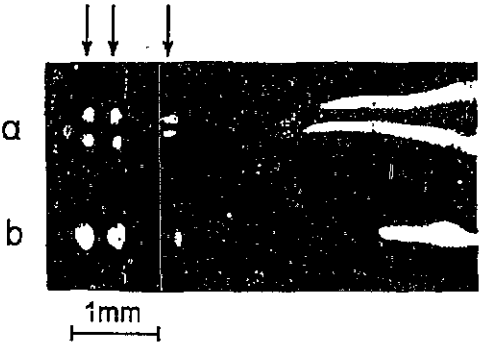

Figure 5. X-ray photographs of the plasma channel obtained in [19] by the x-ray electron–optical image converter. Bright glowing points are ring-wise formations. The interval between the frames is 10 ns.

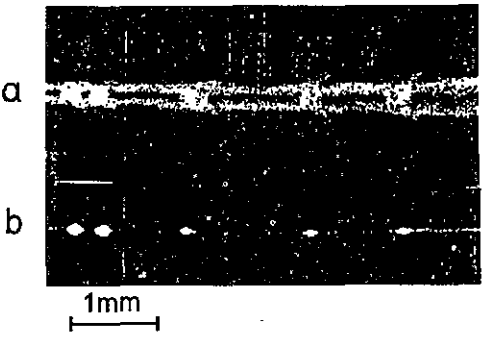

Figure 6. Integral x-ray pinhole photographs obtained in [19] over various spectral ranges.

We think that in the known experiments on micro-pinches [18–20], the discussed self-focusing of current is also realized. Our ideas are supported by the experiments of [19], carried out with the help of an x-ray electron–optical image converter with a time resolution of about 5 ns, which found (by direct observation) that brightly glowing ring formations appear near the maximum of an ultra-soft x-ray radiation (with energy $\leqslant 10$ keV). Over a

time of about 5 ns these formations 'collapse' on the axis (see figure 5). Figure 6, taken from [19], shows integral pinhole photographs of x-ray radiation. One can see that these are mappings of the discharge corona and cross stripes (strata) which superimpose each other. Shadow regions of figure 6 correspond to a 'cold' core, along which a negligibly small part of the current flows. The integral pinhole photographs taken by using filters with a cutoff energy of 2 keV show no corona glow, however one can see hot spots of $\leqslant 80$ μm in size at the points of the axis corresponding to the strata (figure 6(*b*)). The estimation of electron temperature (T_e) in the plasma corona gives 400–800 eV and the estimates of the maximum temperature in hot spots obtained by the absorbing method are 1–2 keV ($T_{max} = (2.5\text{–}5)T_c$, where T_c is the electron temperature in the corona), which is close to the order of magnitude of the estimate of our model (without claim of a better agreement).

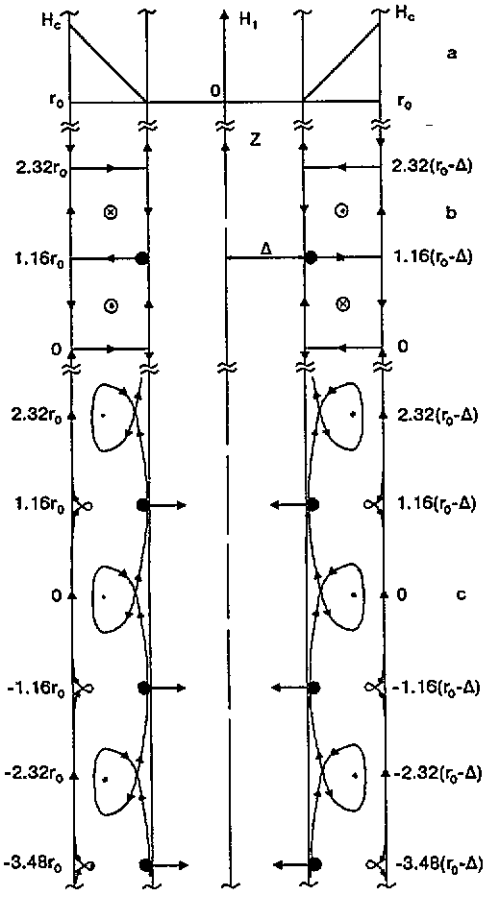

Figure 7. Qualitative picture of 'hot' plasma ring formations in the experiment of [19] according to our model: (*a*) the distribution of the undisturbed magnetic field; (*b*) the cross section of the separatrix surface of the vector velocity field of medium particles in the plane r–z; (*c*) the cross section of the vector velocity field of conduction electrons in the plane r–z. Marked by the bold point symbol is the localization of hot spots in (*a*), (*b*).

It should be noted that in our model the region of high temperature, unlike in experiment [19], localizes on the axis from the very beginning of the process. This is due to the fact that an undisturbed current is distributed uniformly throughout the cylindrical conductor and not along the corona discharge, as in the experiment of [19]. If the above mechanism is taken into account, then in terms of our model, the mechanism of hot-spot formation in the experiments of [19] is easily understood. Figure 9 of paper [2], in this case, corresponds to figure 7, which represents a picture of hot-spot formation. Subsequently, due to the replacement of current from the corona discharge to the core, hot spots localize on the axis.

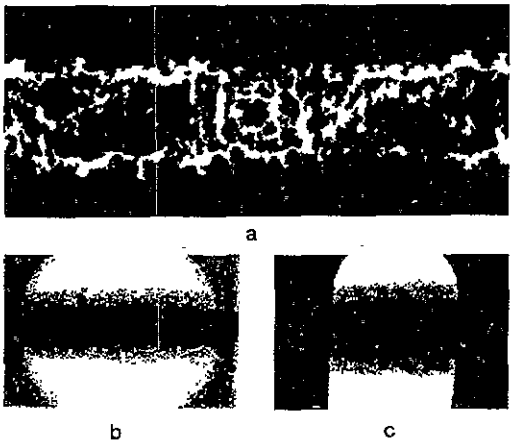

Figure 8. (*a*) Optical image of the exploding conductor and (*b*), (*c*) shadow x-ray pictures obtained in [4] by using the electron–optical image converter and pulse shadow x-ray photography (the exposure time of the optical pattern is 5 ns and of the x-ray pattern 25 ns). The bright glow in (*a*) corresponds to high-velocity jets formed as a result of the escape of overheated matter from the near-axis zone up to conductor surface.

In the process of electric explosion, overheated matter emerges from the near-axis zone up to the surface in the form of bright, high-velocity jets which give rise to an additional high-velocity shock wave in the ambient air [4]. These jets set a typical pattern (figure 8) where the original space period is preserved. Being aware of the velocity of these jets, one can give a lower estimate for the matter temperature in the near-axis zone. For one of the experiments [4] this estimation gives a temperature of 5 eV with a volume average of about 0.5 eV. In the simulation (figure 4(*a*)) the maximum temperature in hot spots is 23 times greater than the average temperature.

The model enables division of the process into definite phases and the formalizing of such widely used notions as the delay time and the switching time. In particular, in experiments with inductive accumulators of power there is a certain typical time when the current reaches its maximum. From this time the current starts decreasing, whereas the Ohmic component of voltage continues increasing. A section of a negative differential resistance appears in the UI-characteristic. This moment is highlighted in our model (circuit S3 in [2]): a topological rearrangement of singular points of the dynamic system defined by equations (6) and (7) of [2] takes place here. As a result of this rearrangement the first system of current vortices is formed and the conductor ceases to be simply connected (the separatrix surface of the current velocity field of conduction electrons divides the conductor into two channels (figure 12 in [2]).

The analysis of the x-ray picture series exhibits that at a certain moment, lying to the right of the current maximum when its value is at the level of 0.8–0.9 from the maximum, a fast process of conductor destruction begins (this process is the phase of commutation). This process is not marked in any way on current and voltage waveforms. However, a fracture on the time dependence of the Kolmogorov–Sinai entropy appears (see figure 5 in [2]) which justifies the division of the process into stages: the initial and final stages of commutation. There is one more typical point, namely the one where the rate of entropy growth reaches its maximum. It occurs at a current amplitude level of 0.1–0.2 of the maximum. It is convenient to connect this moment with the end of the commutation phase.

While other conditions are held constant, the lower the conductivity, the smaller the critical magnetic Rayleigh number. Therefore, the nonlinear effects of transition metals under discussion will be more strongly pronounced than those of materials such as silver and copper, corresponding to experimental observations. In particular, the anomalous dependence of resistance on the absorbed energy in transition metals is more pronounced [4].

4. Conclusion

The results obtained in [1,2] and discussed above are mostly of a qualitative character. As pointed out in [1], they lose applicability from the beginning of the space scale splitting. The sequence of doubling the space scale pointed out in [1]: $k_0 \rightarrow k_1 = 0.5k_0 \rightarrow k_2 = 2k_0 \rightarrow k_3 = 2k_2 \rightarrow k_4 = 2k_3 \rightarrow \cdots$ is peculiarly analogous to the hypothesis of scale invariance in the second-kind phase transition theory [22]. Since our model is a model of a non-equilibrium phase transition, an analogue for the critical point is the magnetic Rayleigh number, where stationary states are absent if the latter is exceeded (see figure 3(a) in [1] presenting the bifurcation curve).

It appears that in order to describe the first stage of splitting and the formation of a low-temperature plasma with a condensed disperse phase ($k_0 \rightarrow k_1$) one can also limit oneself to three modes of perturbation [15]. It has to be noted that the dynamics of the process in this stage are qualitatively similar to the destruction of superconductivity by a critical current [23,24] and therefore it is interesting to construct a model for the destruction of a superconducting state as the model of a non-equilibrium phase transition which occurs as a result of the 'crisis' in the two-liquid magneto-hydrodynamics of the superconductor.

Nevertheless, despite the limitation mentioned, we were able, in terms of our model and the results of simulation, to give a qualitative explanation from a common standpoint to experimental results on the electric explosion of conductors, previously considered anomalous. In particular, the mechanism of localizing heat sources, according to which the formation of hot plasma spots in plasma-like media occurs, not on account of a strong dependence of local kinetic coefficients on the density and temperature (the medium in our model was assumed incompressible with constant kinetic coefficients) and also sausage-type instabilities (pinches), but due to the formation of vortex structures in the system (see figures 7 and 9 in [2]).

Since we have shown the possibility of hot-spot formation in a liquid metal, it has to be expected that hot spots can exist near the cathode surface from the side of the metal and be responsible for the initiation and dynamics of vacuum arc cathode spots [25], the behaviour of which has so far been obscure. In our opinion, hot spots play a leading role in the phenomenon called explosive electron emission, which is widely used in applied physics [26,27].

It should be emphasized that the processes discussed in our series refer to a class of non-equilibrium phase transitions and therefore the simplest model proposed by us (the incompressible plasma-like medium with constant local kinetic coefficients and the three space modes of perturbation) enabled a qualitative understanding of a wide class of experiments including the mechanism of hot spot formation in experiments on micro-pinches [17].

Acknowledgments

We are pleased to thank K Ye Bobrov for assistance in producing the computer drawings for this series.

References

[1] Volkov N B and Iskoldsky A M 1993 *J. Phys. A: Math. Gen.* **26** 6635

[2] Volkov N B and Iskoldsky A M 1993 *J. Phys. A: Math. Gen.* **26** 6649
[3] Lebedev S V and Savvatimsky A I 1985 *Sov. Phys. Usp.* **144** 243
[4] Iskoldsky A M 1985 *Thesis* (Tomsk High Current Electronics Institute) (in Russian)
[5] Boortzev V A, Kalinin N V and Lootchinsky A V 1990 *Electrical Explosion of Conductors and its Use in Electrophysical Devices* (Moskow: Energoatomisdat) (in Russian)
[6] Vichrev V V and Braginsky S I 1980 *Voprosi Teorii Plasmi* vol 10, ed M A Leontovitch (in Russian)
[7] Fillipov N V, Fillipova T I and Vinogradov V L 1962 *Nucl. Fusion Suppl.* part 2
[8] Weber B V *et al* 1987 *IEEE Trans. Plasma Sci.* **PS-15** 635
[9] Baikov A P, Iskoldsky A M and Nesterichin Yu E 1975 *JTF* **45** 136 (in Russian)
[10] Lebedev S V and Savvatimsky A I 1981 *Tepl. Vis. Temp.* **19** 1184 (in Russian)
[11] Abramova K B, Zlatin N A and Peregood B P 1975 *JETF* **69** 2007 (in Russian)
[12] Bodrov S G, Lev M A and Peregood B P 1978 *JTF* **48** 2519 (in Russian)
[13] Kadić A and Edelen D G B 1983 *A Gauge Theory of Dislocations and Disclinations* (Berlin: Springer)
[14] Lamb H 1932 *Hydrodynamics* (Cambridge: Cambridge University Press)
[15] Volkov N B and Iskoldsky A M 1991 *Proc. 8th All-Union Conf. on Physics of Low-Temperature Plasmas* vol 1 (Minsk: Institute of Physics Belorussia Academy of Science) (in Russian)
[16] Frenkel Ja I 1975 *The Kinetic Theory of Liquids* (Leningrad: Nauka) (in Russian)
[17] Korop E D, Meyerovitch B E, Sidelnikov Ju V and Soochorukov O B 1979 *Usp. Fiz. Nauk* **129** 87 (in Russian)
[18] Baksht R B, Datsko I M and Korostelev A F 1985 *JTF* **55** 1540 (in Russian)
[19] Aivazov I K, Arantchook L E, Bogoljubsky S L and Volkov G S 1985 *Pis'ma v JETF* **41** 111 (in Russian)
[20] Baksht R B 1991 Plasmennii stolb, obrasovannii vzrivom microprovodnikov *Preprint N6* Tomsk Institute of High Current Electronics, Russian Academy of Science, Siberia Division (in Russian)
[21] Vichrev V V, Ivanov V V and Koshelev K N 1982 *Fisika Plasmi* **8** 1211 (in Russian)
[22] Ma Shang-keng 1976 *Modern Theory of Critical Phenomena* (Massachusetts: Benjamin)
[23] London F 1937 *Une conception nouvelle de la supraconductivite* (Paris)
[24] Andreev A F 1968 *JETF* **54** 1510 (in Russian)
[25] Mesyats G A and Proskurovsky D I 1989 *Pulsed Electrical Discharge in Vacuum* (Berlin: Springer)
[26] Boogaev S P, Iskoldsky A M, Mesyats G A and Proskurovsky D I 1967 *JTF* **37** 2206 (in Russian)
[27] Foorsey G N and Vorontsov-Vel'yaminov P N 1967 *JTF* **37** 1870 (in Russian)